

Center phase transition from matter propagators in (scalar) QCD

M. Mitter^{a,b}, M. Hopfer^a, B.-J. Schaefer^c, R. Alkofer^a

^a*Institut für Physik, NAWI Graz, Karl-Franzens-Universität Graz, Austria*

^b*Department of Physics, Brookhaven National Laboratory, Upton, NY 11973*

^c*Institut für Theoretische Physik, Justus-Liebig-Universität Gießen, Germany*

Abstract

Novel order parameters for the confinement-deconfinement phase transition of quenched QCD and fundamentally charged scalar QCD are presented. Similar to the well-known dual condensate, they are defined via generalized matter propagators with $U(1)$ -valued boundary conditions. The order parameters are easily accessible with functional methods. Their validity and accessibility is explicitly demonstrated by numerical studies of the Dyson-Schwinger equations for the matter propagators. Even in the case of heavy scalar matter, where the propagator does not show a signature of the phase transition, a discontinuity due to the transition can be extracted in the order parameters, establishing also fundamentally charged scalar matter as a probe for color confinement.

1. Introduction

In the limit of infinitely heavy matter in the fundamental representation of the gauge group, the deconfinement transition in $SU(N)$ gauge theories can be characterized by the breaking and restoration of center symmetry, cf. e.g. Ref. [1]. In the low temperature phase, purely gluonic systems are center symmetric, and the phase transition to a deconfined state is related to the spontaneous breaking of center symmetry. A corresponding order parameter is given by the Polyakov loop

$$L = \langle \text{tr} \mathcal{P} \exp \int_0^\beta dx_0 A_0(x) \rangle, \quad \beta = 1/T, \quad (1)$$

where the trace is taken over the gauge group algebra in the fundamental representation, \mathcal{P} denotes path ordering, and A_0 is the time-like component of the gauge field degrees of freedom. This quantity can be related to the exponential of the negative free energy of a pair of free fundamentally charged matter particles. As a consequence, a vanishing Polyakov loop corresponds to an infinite energy cost for freeing the

matter particles, and is therefore interpreted as an indicator for a confined matter phase. This observation is not restricted to gauge groups with a non-trivial center. Interestingly, for gauge groups with a trivial center, such as the exceptional Lie group G_2 , quenched calculations reveal also a clear evidence for a first-order phase transition [2–7]. Although in this case the Polyakov loop is not an order parameter in the strict sense, it is still sensitive to the phase transition and behaves very similar to its pendant in the $SU(3)$ case.

In the quenched limit of $SU(2)$, one finds a second-order phase transition from a confined to a deconfined phase around a critical temperature of $T_c \approx 230$ – 240 MeV in continuum approaches like the functional renormalization group (FRG) method or the variational Hamiltonian approach [8–10] whereas in numerical lattice simulations $T_c \approx 295$ MeV [11]. In contrast, for $SU(3)$, a first order transition is found at $T_c \approx 275$ MeV in the FRG [9], at $T_c \approx 245$ MeV in the variational Hamiltonian approach [10], and at $T_c \approx 270$ MeV on the lattice [11].

With functional methods like the Dyson-Schwinger

equations (DSEs) and the FRG, see e.g. [12–28] for reviews and [8, 9, 29–42] for investigations of finite temperature Yang-Mills theory and the center-symmetry transition, it is usually hard to access the Polyakov loop directly, see also [43]. Initiated by the pioneering work on spectral sums in lattice gauge theory [44–46], the formulation of order parameters which are accessible to functional methods, has been achieved in the last decade [30, 47, 48]. In particular, this concerns the dual chiral condensate [30]

$$\Sigma_1 = - \int_0^{2\pi} \frac{d\varphi}{2\pi} e^{-i\varphi} \langle \bar{\psi}\psi \rangle_\varphi . \quad (2)$$

which has been successfully applied to the center phase transition in quenched QCD [30, 32, 33] as well as in investigations of the QCD phase structure [31, 34, 35, 38]. It corresponds to a dressed Polyakov loop, i.e. a sum over all loops that wind once around the torus [46]. Therefore it transforms like the Polyakov loop itself under center symmetry.

In this work, we introduce novel order parameters that allow to use fundamentally charged matter as a probe for color confinement in the quenched limit. In particular, we apply a new order parameter for QCD that is based on a condensate, which remains finite even in the case of non-vanishing current quark masses. Furthermore, we investigate scalar QCD, a QCD-like theory where the quarks are substituted by fundamentally charged scalar fields, cf. [49–62] and references therein. It is expected that not only quarks but any fundamentally charged matter is confined [50]. To be more precise, the confined phase of scalar QCD is actually continuously connected to a Higgs-like phase [63–65], however, both “phases” can be distinguished by the infrared saturation of, e.g., the gluon DSE [66]. Nevertheless we will treat (quenched) scalar QCD as if it would experience a confining phase like (quenched) QCD and relate confinement to center symmetry. An advantage of scalar QCD is a drastic simplification of the (finite temperature) tensor structures in the higher n -point functions, particularly in comparison to the quark-gluon vertex [67–73].

This paper is organized as follows: We discuss the construction of order parameters for center symmetry

in Sec. 2. The DSEs for (scalar) QCD and its solution are discussed in Sec. 3 and our numerical results for the matter propagators and order parameters are presented in Sec. 4. We summarize our findings and conclude in Sec. 5.

2. Center-symmetry order parameters

In the following, we consider arbitrary matter fields Φ in the fundamental representation of the gauge group. Applied to a gauge theory at finite temperature with $\beta \equiv 1/T$, the center symmetry transformations of the gauge fields $A_\mu = A_\mu^a T^a$ in the adjoint representation of the gauge group G and the fundamental matter fields Φ read

$$\mathcal{T}_z A_\mu(\vec{x}, x_4 + \beta) = z A_\mu(\vec{x}, x_4) z^\dagger = A_\mu(\vec{x}, x_4) , \quad (3)$$

$$\mathcal{T}_z \Phi(\vec{x}, x_4 + \beta) = z e^{i\varphi} \Phi(\vec{x}, x_4) . \quad (4)$$

Here $z \in Z(G)$ labels the center elements of the gauge group G and \mathcal{T}_z denotes a center-symmetry transformation. For the $SU(3)$ gauge group, for example, the center elements are given by $z \in \{0, e^{i2\pi/3}, e^{i4\pi/3}\}$. In Eq. (4), a general boundary condition $e^{i\varphi} \in U(1)$ has been assumed for the matter field. Hence, the gauge fields in the adjoint representation are invariant, while the matter fields in the fundamental representation pick up a non-trivial phase according to their boundary condition and are thus not invariant under center transformations.

In analogy to Eq. (2), we define a general class of order parameters Σ as the Fourier transform of a condensate Σ_φ , which depends on the generalized φ -valued boundary conditions by

$$\Sigma = \int_0^{2\pi} \frac{d\varphi}{2\pi} e^{-i\varphi} \Sigma_\varphi . \quad (5)$$

The novel order parameters are sensitive to center-symmetry breaking, transform as the conventional Polyakov loop under center transformations, and can be easily extracted from the propagator DSEs. To be an order parameter for the center phase transition, Σ should transform under center transformation as

$$\mathcal{T}_z \Sigma = z \Sigma . \quad (6)$$

To achieve this general transformation property, it is sufficient that the condensate Σ_φ fulfills

$$\Sigma_\varphi = \Sigma_{\varphi+2\pi}, \quad \varphi \in [0, 2\pi[, \quad (7)$$

$$\mathcal{T}_z \Sigma_\varphi = \Sigma_{\varphi+\arg(z)}. \quad (8)$$

The first condition is the closure of the $U(1)$ -valued boundary condition and the second condition utilizes the unit modulus of the center elements, which results in an additive shift of the boundary angle by $\arg(z)$. It is obvious that Eq. (7) and Eq. (8) together with Eq. (5) implies Eq. (6), i.e.

$$\begin{aligned} \mathcal{T}_z \Sigma &= \int_0^{2\pi} \frac{d\varphi}{2\pi} e^{-i\varphi} \Sigma_{\varphi+\arg(z)} \\ &= \int_{\arg(z)}^{2\pi+\arg(z)} \frac{d\hat{\varphi}}{2\pi} e^{-i(\hat{\varphi}-\arg(z))} \Sigma_{\hat{\varphi}} = z \Sigma . \end{aligned} \quad (9)$$

Note that in the derivation of the order parameter no reference to the ordinary Polyakov loop has been used. Only the center-symmetry transformation properties of the condensates, summarized in Eqs. (7) and (8), together with the integrability of the propagator dressing functions have been exploited. The resulting order parameter transforms as the conventional Polyakov loop, cf. Ref. [44]. Thus, the remaining task is the construction of condensates Σ_φ that fulfill Eq. (7) and Eq. (8).

2.1. Order parameter for scalar QCD

The aim is now to find a condensate Σ_φ that fulfills the requirements of (7) and (8) and can be expressed in terms of the scalar propagator $D_{S,\varphi}$. Applying Eq. (4), we see that a center-symmetry transformation changes only the boundary condition of the propagator

$$\mathcal{T}_z D_\varphi(\vec{x}, x_4) = D_{\varphi+\arg(z)}(\vec{x}, x_4). \quad (10)$$

The sought for condensate Σ_φ should therefore be related to the propagator such that it depends only on the boundary condition of the propagator. Hence, we propose for real-valued propagators the condensate

$$\Sigma_\varphi \equiv \int_0^\beta d\tau D_\varphi^2(\vec{p} = \vec{0}, \tau), \quad (11)$$

evaluated at vanishing three-momentum. This expression is obviously periodic in φ with periodicity 2π , since D_φ is invariant under $\varphi \rightarrow \varphi + 2\pi$. The second requirement, (8), is also trivially fulfilled because of (10). Rather than evaluating the propagator at some fixed τ , or integrating over the propagator itself, we choose to integrate over the square of the propagator in Eq. (11). This has the advantage that we can express Σ_φ as a sum over Matsubara modes of the momentum space propagator

$$\Sigma_\varphi = T \sum_n D_\varphi^2(\vec{p} = \vec{0}, \omega_n(\varphi)), \quad (12)$$

with nice convergence properties. From a mathematical point of view this can be understood by analogy to the well-known L^2 -norm.

2.2. Order parameter for QCD

For the construction of a center-symmetry order parameter for QCD, we start from the quark propagator

$$S(\vec{p}, \omega_n) = \frac{-i\gamma^4 \omega_n C - i\vec{\gamma} \cdot \vec{p} A + B}{\omega_n^2 C^2 + \vec{p}^2 A^2 + B^2}. \quad (13)$$

Here, the three dressing functions A , B and C depend on the three-momentum \vec{p} and the Matsubara mode ω_n . We propose the generalized φ -dependent quark condensate

$$\Sigma_\varphi^{(q)} = T \sum_n \left[\frac{1}{4} \text{tr}_D S(\vec{0}, \omega_n(\varphi)) \right]^2, \quad (14)$$

for the construction of a center-symmetry order parameter. In contrast to the conventional quark condensate $\langle \bar{\psi}\psi \rangle_\varphi$ used in Eq. (2), the condensate $\Sigma_\varphi^{(q)}$ is finite even in the case of non-vanishing bare quark masses. Furthermore, we expect a better convergence compared to the dual scalar quark dressing, introduced in Ref. [32].

3. Propagator Dyson-Schwinger equations

3.1. Fundamentally charged scalar QCD

In QCD, the quark fields transform under the fundamental representation of the $SU(3)$ gauge group.

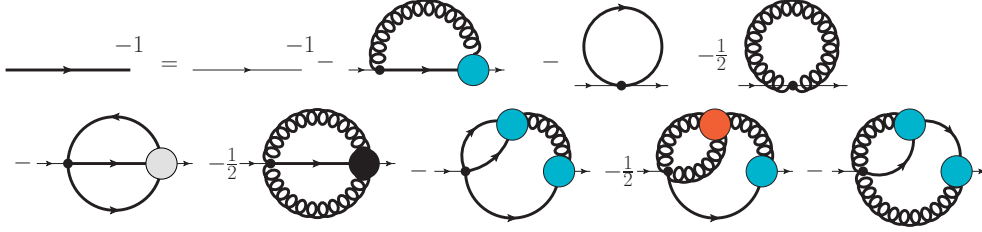


Figure 1: The DSE for the full scalar propagator includes full gluon propagators (curly lines), full (thick colored) and bare (small dots) vertices. See [49] for more details.

A QCD-like theory that seems to be simpler at first glance can be obtained by replacing the quark fields with complex scalar fields that share the same transformation properties under the $SU(3)$ gauge group. This leads to fundamentally charged scalar QCD whose renormalized Euclidean Lagrangian in Landau gauge [49, 50] reads

$$\begin{aligned}
\mathcal{L} = & Z_3 A_\mu^a \left(\frac{1}{2} (-\partial^2 \delta_{\mu\nu} + \partial_\mu \partial_\nu) \right) A_\nu^a \\
& + Z_1 g f^{abc} (\partial_\mu A_\nu^a) A_\mu^b A_\nu^c - \tilde{Z}_1 g f^{abc} \bar{c}^a \partial_\mu (c^b A_\mu^c) \\
& - \tilde{Z}_3 \bar{c}^a \partial^2 c^a + Z_4 \frac{g^2}{4} f^{abc} f^{ade} A_\mu^b A_\nu^c A_\mu^d A_\nu^e \\
& + ig \hat{Z}_{1F} T^a \phi^* (2A_\mu^a (\partial_\mu \phi) + (\partial_\mu A_\mu^a) \phi) \\
& + \hat{Z}_4 \frac{\lambda}{4} (\phi^* \phi)^2 + \phi^* \hat{Z}_2 (-\partial^2 + Z_m m^2) \phi \\
& + \frac{\hat{Z}_{4,2}}{2} \{T^a, T^b\} g^2 \phi^* A_\mu^a A_\mu^b \phi .
\end{aligned} \tag{15}$$

The gluon fields with the gauge coupling g are denoted by A_μ^a , the (anti)ghosts fields by (\bar{c}^a, c^a) and the fundamentally charged scalar fields by ϕ . Besides the coupling to the gauge sector, renormalizability allows for a mass term m and a quartic coupling λ in the scalar sector. Furthermore, the gauge invariant coupling of the scalars to the glue sector implies the presence of a two-scalar-two-gluon vertex. Compared to ordinary QCD, scalar QCD has therefore two additional bare vertices, which results in a richer diagrammatic structure of the corresponding DSEs. In particular, this compensates to some extent the simplifications that are gained by replacing Dirac spinors with scalar fields. All primitively divergent vertices are endowed with renormalization constants. Sim-

ilarly to QCD, these are related by Slavnov-Taylor identities like $Z_3/Z_1 = \tilde{Z}_3/\tilde{Z}_1$ [74], where $\tilde{Z}_1 = 1$, and therefore $\hat{Z}_{1F} = \hat{Z}_2/\tilde{Z}_3$, in Landau gauge [75].

3.2. Scalar propagator Dyson-Schwinger equation

The DSE for the inverse scalar propagator $D_S^{-1}(p)$ is depicted in Fig. 1. Due to the presence of bare four-point functions that involve the scalar field, its structure is considerably more complicated than the corresponding DSE for the quark propagator. Since our investigation focuses on the application of a new order parameter for scalar QCD we use a truncated version of the propagator equation in this work. The contribution from the additional two-loop diagrams is suppressed in the coupling in the ultraviolet. Furthermore, all but two of the two-loop diagrams are additionally suppressed in the scalar mass, which is chosen to be of order GeV. We found that too small masses for the scalar field lead to instabilities in the numerical solution, most likely due to the vertex model or missing diagrams. For the purpose of this work this large value for the mass is no restriction, since its main effect is the suppression of matter backreactions, which is the definition of the quenched limit investigated here. Hence, major contributions from the two-loop diagrams, which are neglected completely, are expected only in the mid-momentum regime. The main effect of the tadpole diagrams, on the other hand, is a shift of the mass counterterm of the scalar propagator, which has no significant impact on the results. Their non-perturbative contribution is likely to be small compared to the error already induced by the missing two-loop diagrams, see also Ref. [76] for an investigation of the

tadpole diagram in the gluon DSE. As a consequence, the tadpoles can safely be ignored as well and the resulting DSE is of the same diagrammatic structure as the one for the quark propagator. The truncated scalar propagator DSE is therefore finally given by

$$D_S^{-1}(p) = \hat{Z}_2 \left(p^2 + \hat{Z}_m m_0^2 \right) - g^2 C_F \hat{Z}_{1F} \times \int \frac{d^4 q}{(2\pi)^4} (p+q)^\mu D^{\mu\nu}(k) D_S(q) \Gamma^\nu(q, p). \quad (16)$$

with the Casimir invariant $C_F = (N_c^2 - 1)/(2N_c)$ and $k = p - q$. The dressed gluon ($D_{\mu\nu}$) and scalar (D_S) propagators are parametrized by

$$D_S(p) = \frac{Z_S(p^2)}{p^2}, \quad D^{\mu\nu}(p) = \frac{Z(p^2)}{p^2} P^{\mu\nu}(p), \quad (17)$$

where the transverse projector $P^{\mu\nu}(p) = \delta^{\mu\nu} - p^\mu p^\nu / p^2$ has been introduced. The reduced scalar-gluon vertex $\Gamma^\mu(p, q)$ is defined by

$$\Gamma_a^\mu(p, q, k) = g T_a (2\pi)^4 \delta^{(4)}(p+k-q) \Gamma^\mu(p, q). \quad (18)$$

The general ansatz for the reduced vertex function contains two dressing functions A' and B' [77, 78]

$$\Gamma^\mu(p, q) = A'(p^2, q^2; \xi)(p+q)^\mu + B'(p^2, q^2; \xi) \left(p^\mu [q^2 - p \cdot q] + q^\mu [p^2 - p \cdot q] \right) \quad (19)$$

with the abbreviation $\xi = p \cdot q / \sqrt{p^2 q^2}$. With these definitions the DSE for the scalar propagator, Eq. (16), can be expressed in terms of the dressing functions

$$Z_S^{-1}(x) = \hat{Z}_2 \left(1 + \hat{Z}_m \frac{m_0^2}{x} \right) - \hat{Z}_{1F} C_F \alpha(\mu) \frac{2}{\pi^2} \int_0^\infty dy y Z_S(y) \mathcal{K}(x, y), \quad (20)$$

where

$$\mathcal{K}(x, y) = \int_{-1}^1 d\xi (1 - \xi^2)^{3/2} \frac{Z(z)}{z} \times \left\{ \frac{A'(y, x; \xi)}{z} + \frac{B'(y, x; \xi)}{2} \right\}. \quad (21)$$

Here, $x = p^2$, $y = q^2$ and $z = x + y - 2\sqrt{xy}\xi \equiv k^2$ denote the squared external and internal scalar and gluon momenta, respectively. The renormalized gauge coupling $\alpha(\mu) = g^2(\mu)/(4\pi)$ is evaluated at the renormalization scale μ .

The generalization of the scalar propagator DSE to finite temperatures is done within the Matsubara formalism with generalized $U(1)$ -valued boundary conditions, where the fourth momentum component is replaced by discrete Matsubara frequencies

$$p_4 \rightarrow \omega_n(\varphi) = (2\pi n + \varphi)T \text{ with } n \in \mathbb{Z}. \quad (22)$$

Consequently, the momentum integral in the p_4 direction is replaced by a sum over the discrete Matsubara modes. For periodic boundary conditions, i.e. $\varphi = 0$, bosonic Matsubara frequencies are used. Since the heat bath explicitly breaks Lorentz symmetry, the scalar propagator dressing is now a function of the spatial momentum \vec{p} as well as the Matsubara frequency ω_n ,

$$D_S(\vec{p}, \omega_n) = \frac{Z_S(\vec{p}^2, \omega_n)}{\omega_n^2 + \vec{p}^2}. \quad (23)$$

The gluon propagator dressing splits into an electric (L) and a magnetic (T) component, which are longitudinal and transverse to the heat bath,

$$D^{\mu\nu}(p) = P_L^{\mu\nu}(p) \frac{Z_L(p)}{p^2} + P_T^{\mu\nu}(p) \frac{Z_T(p)}{p^2}, \quad (24)$$

with the projection operators $P_L^{\mu\nu} = P^{\mu\nu} - P_T^{\mu\nu}$ and $P_T^{\mu\nu}(p) = \delta^{i\mu} \delta^{i\nu} (\delta^{ij} - p^i p^j / \vec{p}^2)$. Although the vertex would admit a similar splitting, we will ignore this possibility for simplicity and employ a degenerate vertex dressing for the electric and magnetic components of the scalar-gluon vertex. Since we are using a model for the vertex anyway, we will use the model parameter to fix its overall effect to the physically required result. The consequences of choosing a vertex model are discussed further in the results section. Thus, the finite temperature DSE can immediately

T/T_c	0	0.361	0.44	0.451	0.549	0.603	0.733	0.903	0.968	0.986	1	1.02	1.04	1.1	1.81	2.2
$a_L(T)$	0.60	0.42	0.23	0.33	0.19	0.17	0.11	0.098	0.082	0.079	0.16	0.27	0.32	0.50	2.71	4.72
$b_L(T)$	1.36	1.23	1.14	1.20	1.13	1.08	1.10	1.13	1.14	1.14	1.05	1.05	1.03	1.07	1.14	1.47
$a_T(T)$	0.60	0.71	0.78	0.83	0.86	1.04	1.05	1.67	1.57	1.06	0.54	0.55	0.57	0.63	1.47	1.42
$b_T(T)$	1.36	1.37	1.46	1.47	1.52	1.60	1.60	1.91	1.81	1.45	1.13	1.14	1.17	1.19	1.49	1.30

Table 1: The fit parameters for the temperature dependent SU(3) gluon propagator, adopted from [33].

be inferred from Eq. (16), leading to

$$\hat{Z}_2^{-1} Z_S^{-1}(x, \omega_m) = 1 + \hat{Z}_m \frac{m^2}{\omega_m^2 + x} - \frac{C_F \alpha(\mu)}{2\pi} \times T \sum_{n \in \mathbb{Z}} \int_0^\infty dy \sqrt{y} \frac{Z_S(y, \omega_n)}{\omega_n^2 + y} \mathcal{A}(x, \omega_m, y, \omega_n), \quad (25)$$

with

$$\mathcal{A}(x, \omega_m, y, \omega_n) = \frac{4}{\omega_m^2 + x} \int_{-1}^1 d\xi \left\{ \frac{Z_L(k^2)}{k^2} \times \frac{(\omega_m^2 + x)(\omega_n^2 + y) - (\omega_m \omega_n + \sqrt{xy} \xi)^2}{k^2} + \frac{Z_T(k^2) - Z_L(k^2)}{k^2} \frac{xy(1 - \xi^2)}{\bar{k}^2} \right\} \times A(x, \omega_m^2, y, \omega_n^2; \xi), \quad (26)$$

where $\bar{k}^2 = x + y - 2\sqrt{xy} \xi$ are now the corresponding spatial momenta and $k^2 = (\omega_m - \omega_n)^2 + \bar{k}^2$.

3.3. Gluon propagator

One important ingredient for the numerical treatment of the matter propagator DSEs is the temperature-dependent gluon propagator. A self-consistent incorporation of the corresponding Yang-Mills DSEs is beyond the scope of this work. Therefore, we proceed analogously to previous works, see e.g. Refs. [30, 32, 33], and use lattice results to fit the gluon propagator. For the two dressings in Eq. (24),

the following fit function is employed [33]

$$Z_{T,L}(q, T) = \frac{q^2 \Lambda^2}{(q^2 + \Lambda^2)^2} \left\{ \left(\frac{c}{q^2 + a_{T,L} \Lambda^2} \right)^{b_{T,L}} + \frac{q^2}{\Lambda^2} \left(\frac{\beta_0 \alpha(\mu) \ln [q^2/\Lambda^2 + 1]}{4\pi} \right)^\gamma \right\}. \quad (27)$$

Here $c = 11.5 \text{ GeV}^2$ and the anomalous dimension is $\gamma = -13/22$. The renormalization scale is fixed to $\alpha(\mu) = 0.3$ and $\beta_0 = 11N_c/3$ is the universal β -function coefficient of the quenched theory. The temperature-independent scale parameter $\Lambda = 1.4 \text{ GeV}$ reflects the gapping scale of the gauge sector of the theory. The temperature-dependent parameters $a_{T,L}$ and $b_{T,L}$ for the magnetic and electric dressing functions are used to fit the different temperature dependence in the magnetic and electric gluon propagators and listed in Tab. 1.

3.4. Scalar-gluon vertex

For the complete numerical solution of the Dyson-Schwinger equation for the scalar propagator the scalar-gluon vertex is also needed. Since the DSE for the scalar propagator, Eq. (20), depends only on the sum of the two dressing functions that define the scalar-gluon vertex, Eq. (19), it is sufficient to provide only one model dressing function. The construction of the model dressing functions A is done analogous to the very successful model dressing functions used for the quark-gluon vertex in investigations of the QCD phase structure [33] and reads explicitly

$$A(x, y; \xi) = \tilde{Z}_3 \frac{D_S^{-1}(x) - D_S^{-1}(y)}{x - y} d_1 \times \left\{ \left(\frac{\Lambda^2}{\Lambda^2 + z} \right) + \frac{z \beta_0}{\Lambda^2 + z} \left(\frac{\alpha(\mu) \ln [\frac{z}{\Lambda^2} + 1]}{4\pi} \right)^{2\delta} \right\}. \quad (28)$$

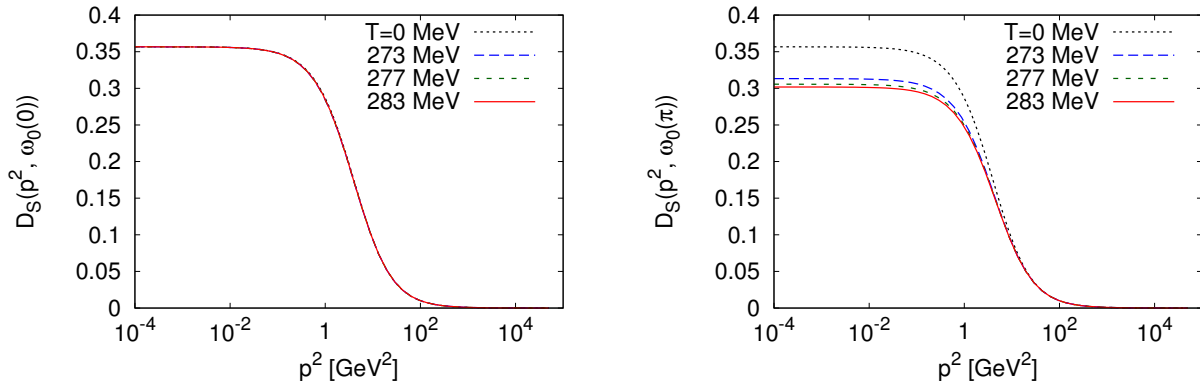


Figure 2: Scalar propagator, Eq. (25), for periodic $\omega_0(0) = 0$ (left) and for antiperiodic $\omega_0(\pi) = \pi T$ (right) boundary conditions as a function of momenta for different temperatures ($\mu = 4$ GeV and $m = 1.5$ GeV).

Again, $x = p^2$, $y = q^2$ and $z = x + y - 2\sqrt{xy}\xi \equiv k^2$ denote the squared external and internal scalar and gluon momenta, respectively. The multiplication with the propagator-dependent function is derived from Ward identities of scalar electrodynamics and represents a generalization of the Ball-Chiu vertex [77, 78]. Together with the anomalous dimension $2\delta = -18/44$ and the values of β_0 and $\alpha(\mu)$ defined in the previous section, it guarantees the one-loop consistent running of the model dressing function in the perturbative ultraviolet regime [79]. The remaining part of the dressing function is purely phenomenological. In particular, the parameter $d_1 = 0.53$ is introduced to model vertex effects that keep the order parameter as close to zero as possible, as required in the confining phase below the transition temperature. The scale Λ models the transition to the non-perturbative regime of the theory, characterised by the gapping scale of the glue sector. Finally, the vertex is multiplied with \tilde{Z}_3 in order to replace \hat{Z}_{1F} with \hat{Z}_2 in Eq. (20).

At finite temperature we use the same model for the vertex with

$$A(x, \omega_m^2, y, \omega_n^2; \xi) = A(x + \omega_m^2, y + \omega_n^2; \xi).$$

In order to avoid singularities that could arise due to

numerical inaccuracies in the case

$$\begin{aligned} \omega_m^2 + \vec{p}^2 &= \omega_n^2 + \vec{q}^2, \quad \vec{q} \neq \vec{p}, \\ D_S(\vec{p}^2, \omega_m) &\neq D_S(\vec{q}^2, \omega_n), \end{aligned} \quad (29)$$

the vacuum propagator in Eq. (28) is used also at finite temperature.

3.5. Renormalization

At finite temperature, as well as in the vacuum, the divergent self-energy term is regularized with a sharp cutoff, where a four-dimensional cutoff is used, i.e. $x \leq \Lambda_c^2$ in the vacuum and $\omega_n^2 + x \leq \Lambda_c^2$ at finite temperatures with $\Lambda_c^2 = 5 \times 10^4$ GeV². We choose the renormalization scale and conditions such that the counterterms remain unaffected by the introduction of temperature. The self-energy term does not contribute to $\hat{Z}_m m_0^2$ at vanishing momentum and no quadratic divergencies are present in our truncation. Hence, for the determination of the renormalization constant \hat{Z}_m we fix the value of the propagator at vanishing momentum via the (cutoff-dependent) condition $m^2 \equiv [\hat{Z}_{1F} D_S(0)]^{-1} = \hat{Z}_m m_0^2$. In order to fix \hat{Z}_2 , we demand for $\mu^2 > \Lambda_c^2$ that the propagator is proportional to the free massless one, $D_S(\mu^2) = 1/\mu^2$, which in turn yields $\hat{Z}_2 = \mu^2 (\mu^2 + \mu^2 \Pi(\mu^2) + m^2)^{-1}$. This

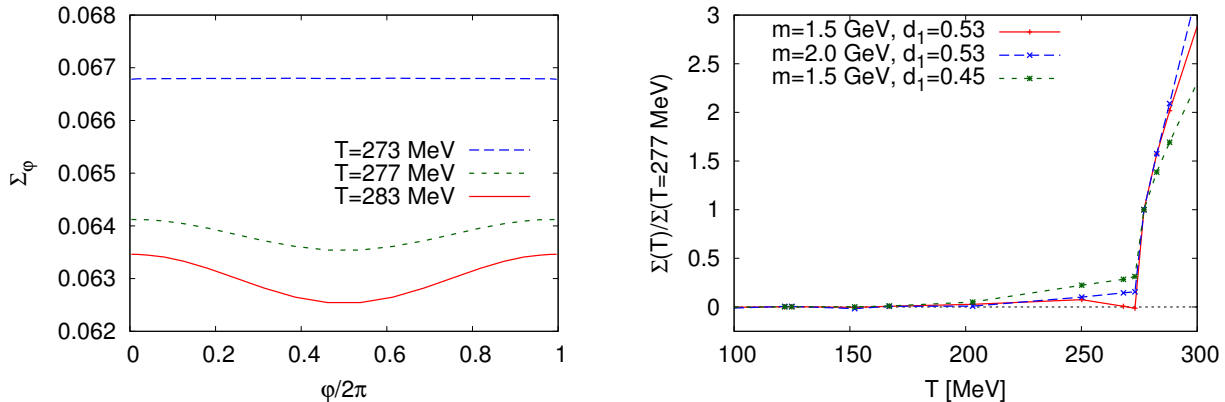


Figure 3: Left panel: Scalar function Σ_φ , Eq. (12), as a function of the boundary conditions for different temperatures ($\mu = 4$ GeV and $m = 1.5$ GeV). Right panel: Normalized scalar condensate as a function of the temperature for different scalar masses m and fit parameter d_1 for the scalar-gluon vertex Eq. (28).

prescription together with the vertex in (28) ensures multiplicative renormalizability in the sense that $\hat{Z}_2(\mu^2, \Lambda_c^2)Z_S(x, \mu^2) = \hat{Z}_2(\tilde{\mu}^2, \Lambda_c^2)Z_S(x, \tilde{\mu}^2)$ for another scale $\tilde{\mu}$.

3.6. Quark propagator Dyson-Schwinger equation

In addition to the center-symmetry order parameters calculated with the scalar propagator in scalar QCD, we also present results for the corresponding order parameters in QCD with quarks. The DSE for the quark propagator and its solution have been discussed in great detail in many previous works, see in particular [33]. Since we evaluate the order parameters on top of the results for the quark propagator already presented therein, we refrain from repeating the corresponding details.

4. Numerical results

We begin our investigation with the numerical solution of the scalar propagator DSE (25), using a temperature-dependent gluon propagator from lattice simulations as input, cf. Sec. 3.3.

In Fig. 2 the scalar dressing function D_S , Eq. (23), is shown as a function of the momentum for different temperatures. The left panel shows the propagator at the lowest periodic Matsubara frequency

$\omega_{n=0}(0) = 0$ and the right panel for the lowest antiperiodic Matsubara frequency $\omega_{n=0}(\pi) = \pi T$. In the case of periodic boundary conditions, the scalar propagator is virtually temperature independent, even above the phase transition temperature $T_c = 277$ MeV. For antiperiodic boundary conditions, on the other hand, a trivial effect is induced by the temperature-dependent lowest Matsubara frequency $\omega_{n=0}(\pi) = \pi T$. Independent of the boundary conditions, it is therefore hard to extract any useful information about the transition temperature from the propagator directly. This temperature insensitivity can be explained by the relatively large scalar mass of $m \sim \mathcal{O}(1)$ GeV in comparison to the transition temperature $T \sim \mathcal{O}(0.1)$ GeV. Consequently, the scalar field is too heavy to be excited by the fluctuations near the phase transition.

We show the condensate Σ_φ , defined in Eq. (12), in Fig. 3, left panel, and find immediately that it is indeed periodic in the $U(1)$ -valued boundary conditions. Below the transition temperature, Σ_φ is φ -independent which in turn results in a vanishing of the order parameter Σ . Above the transition temperature, on the other hand, Σ_φ develops a minimum around $\varphi = \pi$. This leads to a lowered negative contribution in Σ , yielding ultimately an overall non-vanishing positive value for the order parameter.

For periodic boundary conditions, we also find that $\Sigma_{\varphi=0}$ rises after a small dip above T_c rather quickly with the temperature. On the other hand, the large-temperature growth of $\Sigma_{\varphi=\pi}$ is more moderate, leading to an overall increase of the order parameter. In general, this behaviour is similar to the one found in the literature, e.g., with spectral sums of the Dirac-Wilson operator [47], the dual quark condensate evaluated on the lattice [46] or with functional methods [30–33]. In the right panel of Fig. 3, the scalar order parameter is displayed as a function of temperature for two different scalar masses m and different model parameters d_1 for the scalar-gluon vertex. We observe small fluctuations of the order parameter about the required zero value below the transition temperature. These fluctuations are most likely caused by statistical errors in the lattice data. Additionally, we see that, depending on the parameter d_1 in the vertex model, a small but visible unphysical growth or decline in the order parameter can be induced below the critical temperature, where the discontinuity of the phase transition occurs. Nevertheless, we observe a distinct phase transition, which could not be seen in the propagator itself. We conclude that Eq. (5) with (12) is a valid order parameter construction. In contrast, we could not find a linear propagator formulation which emphasizes the importance of the L^2 -convergence property once more.

To confirm that Eq. (14) defines an order parameter for the center phase transition in QCD, we present results for $\Sigma_{\varphi}^{(q)}$ and Σ_q from a self-consistent treatment of the quark propagator DSE in an analogous setup to Ref. [33], cf. Refs. [30, 32]. In the left panel of Fig. 4, the quark condensates $\langle\bar{\psi}\psi\rangle_{\varphi}$ and $\Sigma_{\varphi}^{(q)}$, defined in Eq. (14), are plotted as a function of the boundary angle φ . Both quantities show a similar qualitative behaviour, in particular they are periodic in $\varphi \in [0, 2\pi[$ and symmetric under $\varphi \rightarrow -\varphi$. Below the critical temperature T_c (dashed lines in the figure), the overall values are non-vanishing and positive, whereas a sudden drop occurs above T_c (solid lines). Additionally a flat plateau is formed near antiperiodic boundary conditions in the chiral limit. The corresponding order parameters Σ_1 and Σ_q are

of Fig. 4. Similar to scalar QCD, artefacts due to the statistical error in the lattice simulations as well as a dependence on the vertex model are visible below T_c . In fact, we found a stronger dependence on the vertex model parameter than in the scalar case. This can be explained by the small mass of the quark field in comparison to the scalar theory, since the quark-gluon interaction shows a more pronounced nonperturbative momentum dependence in the case of small quark masses [68]. It is also already clear from purely theoretical considerations that the transition will only become more pronounced and stable against non-perturbative effects in the quark-gluon interaction with growing quark mass. With growing mass the quarks turn into static fundamental sources, whose interaction with the gauge field is determined by the perturbative quark-gluon vertex strength. The behaviour of Σ_q below the phase transition could be improved by varying the model parameters of the quark-gluon vertex. This relatively strong parameter dependence motivates a more detailed investigation of the vertex at finite temperature, cf. [52, 57]. Above the critical temperature, Σ_q seems to flatten out towards higher temperatures, which is in contrast to the dual quark condensate Σ_1 that shows an almost linear growth in the broken center symmetry phase.

5. Summary and conclusions

In this letter we have presented novel order parameters for the confinement-deconfinement phase transition of quenched QCD and scalar QCD. These order parameters are sensitive to the spontaneous breaking of center symmetry, which can be related to confinement in terms of the free energy of quarks and scalars. Similar to the well-known dual condensate, we have defined them as the first Fourier series coefficient of generalized condensates that are determined from matter propagators with $U(1)$ -valued boundary conditions. In particular, we introduced a new order parameter for QCD that is based on a quark propagator dependent condensate, which remains finite even in the case of non-vanishing current quark masses.

These order parameters are easily accessible with functional methods, which are usually based on the expansion of the generating functionals in terms of

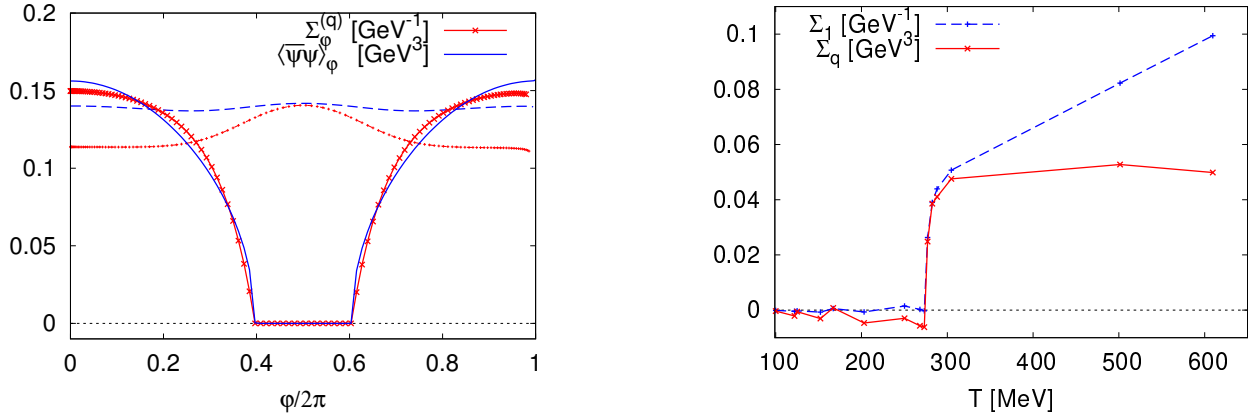


Figure 4: Left panel: Quark $\langle \bar{\psi}\psi \rangle_\varphi$ and dual condensate $\Sigma_\varphi^{(q)}$, Eq. (14), as a function of the $U(1)$ -valued boundary conditions in the chiral limit for temperatures above and below the critical temperature $T_c = 277$ MeV (dashed $T = 273$ MeV, solid $T = 283$ MeV). Right panel: Order parameters Σ_1 , Eq. (2), and Σ_q , Eq. (14) as a function of the temperature.

correlators. Both order parameters rely basically on the L^2 -norm which guarantees excellent convergence properties. We confirmed their validity and accessibility in explicit numerical calculations of the matter propagators by solving the corresponding (truncated) Dyson-Schwinger equations. In particular, we find that even in the case of very heavy scalar matter, where the propagator itself shows no visible signature of a phase transition, the discontinuity related to the phase transition can be extracted. Therefore, these order parameters establish fundamentally charged static scalars, in particular in terms of their propagators, as a probe for color confinement.

Acknowledgments

We thank F. Bruckmann, C.S. Fischer, L. Fister, M. Huber, A. Maas, V. Mader, J. M. Pawłowski, L. von Smekal and A. Windisch for valuable discussions. M.M. acknowledges support from the FWF through DK-W1203-N16 and Erwin-Schrödinger-Stipendium No. J3507-N27, the Helmholtz Alliance HA216/EMMI, the BMBF grant OSPL2VHCTG, the grant ERC-AdG-290623, the DFG grant MI 2240/1-1 and the U.S. Department of Energy under contract de-sc0012704. M.H. acknowledges support from the FWF through DK-W1203-N16. B.-J.S.

acknowledges support by the FWF grant P24780-N27 and by the German Federal Ministry of Education and Research (BMBF) under Contract No. 05P15RGFCA and the Helmholtz International Center for FAIR within the LOEWE program of the State of Hesse.

References

- [1] L. D. McLerran and B. Svetitsky, Phys. Rev. D **24**, 450 (1981).
- [2] M. Pepe and U.-J. Wiese, Nucl.Phys. **B768**, 21 (2007).
- [3] J. Greensite, K. Langfeld, S. Olejnik, H. Reinhardt, and T. Tok, Phys.Rev. **D75**, 034501 (2007).
- [4] G. Cossu, M. D’Elia, A. Di Giacomo, B. Lucini, and C. Pica, JHEP **0710**, 100 (2007).
- [5] J. Danzer, C. Gatttringer, and A. Maas, JHEP **0901**, 024 (2009).
- [6] A. Maas, L. von Smekal, B. H. Wellegehausen, and A. Wipf, Phys.Rev. **D86**, 111901 (2012).
- [7] A. Maas and B. H. Wellegehausen, PoS **LATTICE2012**, 080 (2012).

- [8] J. Braun, H. Gies, and J. M. Pawłowski, *Phys.Lett.* **B684**, 262 (2010).
- [9] L. Fister and J. M. Pawłowski, *Phys.Rev.* **D88**, 045010 (2013).
- [10] H. Reinhardt, *Phys. Rev.* **D94**, 045016 (2016).
- [11] B. Lucini and M. Panero, *Phys. Rept.* **526**, 93 (2013).
- [12] R. Alkofer and L. von Smekal, *Phys.Rept.* **353**, 281 (2001).
- [13] C. D. Roberts and S. M. Schmidt, *Prog. Part. Nucl. Phys.* **45**, S1 (2000).
- [14] C. S. Fischer, *J.Phys.* **G32**, R253 (2006).
- [15] A. C. Aguilar, D. Binosi, and J. Papavassiliou, *Phys. Rev.* **D78**, 025010 (2008).
- [16] C. S. Fischer, A. Maas, and J. M. Pawłowski, *Annals Phys.* **324**, 2408 (2009).
- [17] D. Binosi and J. Papavassiliou, *Phys. Rept.* **479**, 1 (2009).
- [18] A. Maas, *Phys.Rept.* **524**, 203 (2013).
- [19] P. Boucaud, J. P. Leroy, A. L. Yaouanc, J. Micheli, O. Pene, and J. Rodriguez-Quintero, *Few Body Syst.* **53**, 387 (2012).
- [20] G. Eichmann, H. Sanchis-Alepuz, R. Williams, R. Alkofer, and C. S. Fischer, *Prog. Part. Nucl. Phys.* **91**, 1 (2016).
- [21] D. F. Litim and J. M. Pawłowski, in *The exact renormalization group* (Faro, Portugal, 1998), pp. 168–185, [arXiv:hep-th/9901063 \[hep-th\]](#),
- [22] J. Berges, N. Tetradis, and C. Wetterich, *Phys. Rept.* **363**, 223 (2002).
- [23] J. M. Pawłowski, *Annals Phys.* **322**, 2831 (2007).
- [24] H. Gies, *Lect. Notes Phys.* **852**, 287 (2012).
- [25] B.-J. Schaefer and J. Wambach, *Phys. Part. Nucl.* **39**, 1025 (2008).
- [26] O. J. Rosten, *Phys. Rept.* **511**, 177 (2012).
- [27] J. Braun, *J. Phys.* **G39**, 033001 (2012).
- [28] L. von Smekal, *Nucl. Phys. Proc. Suppl.* **228**, 179 (2012).
- [29] F. Marhauser and J. M. Pawłowski, [arXiv:0812.1144 \[hep-ph\]](#).
- [30] C. S. Fischer, *Phys.Rev.Lett.* **103**, 052003 (2009).
- [31] J. Braun, L. M. Haas, F. Marhauser, and J. M. Pawłowski, *Phys.Rev.Lett.* **106**, 022002 (2011).
- [32] C. S. Fischer and J. A. Mueller, *Phys.Rev.* **D80**, 074029 (2009).
- [33] C. S. Fischer, A. Maas, and J. A. Mueller, *Eur.Phys.J.* **C68**, 165 (2010).
- [34] C. S. Fischer, J. Luecker, and J. A. Mueller, *Phys.Lett.* **B702**, 438 (2011).
- [35] C. S. Fischer and J. Luecker, *Phys.Lett.* **B718**, 1036 (2013).
- [36] L. M. Haas, R. Stiele, J. Braun, J. M. Pawłowski, and J. Schaffner-Bielich, *Phys.Rev.* **D87**, 076004 (2013).
- [37] C. S. Fischer, L. Fister, J. Luecker, and J. M. Pawłowski, *Physics Letters B* **732**, 273 (2014).
- [38] C. S. Fischer, J. Luecker, and C. A. Welzbacher, *Phys. Rev.* **D90**, 034022 (2014).
- [39] M. Quandt and H. Reinhardt, *Phys. Rev.* **D92**, 025051 (2015).
- [40] U. Reinosa, J. Serreau, M. Tissier, and A. Tresmontant, *Phys. Rev.* **D95**, 045014 (2017).
- [41] M. Q. Huber, *EPJ Web Conf.* **137**, 07009 (2017).
- [42] A. K. Cyrol, M. Mitter, J. M. Pawłowski, and N. Strodthoff, [arXiv:1708.03482 \[hep-ph\]](#).
- [43] T. K. Herbst, J. Luecker, and J. M. Pawłowski, [arXiv:1510.03830 \[hep-ph\]](#).
- [44] C. Gatttringer, *Phys.Rev.Lett.* **97**, 032003 (2006).
- [45] F. Bruckmann, C. Gatttringer, and C. Hagen, *Phys.Lett.* **B647**, 56 (2007).
- [46] E. Bilgici, F. Bruckmann, C. Gatttringer, and C. Hagen, *Phys.Rev.* **D77**, 094007 (2008).
- [47] F. Synatschke, A. Wipf, and C. Wozar, *Phys.Rev.* **D75**, 114003 (2007).
- [48] F. Synatschke, A. Wipf, and K. Langfeld, *Phys.Rev.* **D77**, 114018 (2008).
- [49] L. Fister, Ph.D. thesis, Heidelberg U. (2009), [arXiv:1002.1649 \[hep-th\]](#),

- [50] L. Fister, R. Alkofer, and K. Schwenzer, *Phys.Lett.* **B688**, 237 (2010).
- [51] V. Macher, A. Maas, and R. Alkofer, *Int.J.Mod.Phys.* **A27**, 1250098 (2012).
- [52] M. Q. Huber and M. Mitter, *Comput.Phys.Commun.* **183**, 2441 (2012).
- [53] A. Maas, *Mod. Phys. Lett.* **A28**, 1350103 (2013).
- [54] M. Mitter, Ph.D. thesis, Graz U. (2012), INSPIRE-1417170;
- [55] M. Hopfer, M. Mitter, B.-J. Schaefer, and R. Alkofer, *Acta Phys.Polon.Supp.* **6**, 353 (2013).
- [56] M. Mitter, M. Hopfer, B.-J. Schaefer, and R. Alkofer, *PoS ConfinementX*, 195 (2012).
- [57] M. Hopfer and R. Alkofer, *Acta Phys.Polon.Supp.* **6**, 929 (2013).
- [58] A. Maas and T. Mufti, *JHEP* **04**, 006 (2014).
- [59] A. Maas and T. Mufti, *Phys. Rev.* **D91**, 113011 (2015).
- [60] M. Hopfer, Ph.D. thesis, Graz U. (2014), INSPIRE-1417166;
- [61] A. Maas, *Eur. Phys. J.* **C76**, 366 (2016).
- [62] A. Maas and P. Torek, *Phys. Rev.* **D95**, 014501 (2017).
- [63] K. Osterwalder and E. Seiler, *Annals Phys.* **110**, 440 (1978).
- [64] R. Bertle, M. Faber, J. Greensite, and S. Olejnik, *Phys.Rev.* **D69**, 014007 (2004).
- [65] K. Langfeld, *AIP Conf.Proc.* **756**, 133 (2005).
- [66] V. Mader, M. Schaden, D. Zwanziger, and R. Alkofer, *Eur. Phys. J.* **C74**, 2881 (2014).
- [67] R. Alkofer, C. S. Fischer, F. J. Llanes-Estrada, and K. Schwenzer, *Annals Phys.* **324**, 106 (2009).
- [68] R. Williams, *Eur. Phys. J.* **A51**, 57 (2015).
- [69] M. Mitter, J. M. Pawłowski, and N. Strodthoff, *Phys. Rev.* **D91**, 054035 (2015).
- [70] R. Williams, C. S. Fischer, and W. Heupel, *Phys. Rev.* **D93**, 034026 (2016).
- [71] D. Binosi, L. Chang, J. Papavassiliou, S.-X. Qin, and C. D. Roberts, *Phys. Rev.* **D95**, 031501 (2017).
- [72] A. C. Aguilar, J. C. Cardona, M. N. Ferreira, and J. Papavassiliou, *Phys. Rev.* **D96**, 014029 (2017).
- [73] A. K. Cyrol, M. Mitter, J. M. Pawłowski, and N. Strodthoff, [arXiv:1706.06326](https://arxiv.org/abs/1706.06326) [[hep-ph](https://arxiv.org/archive/hep)].
- [74] W. J. Marciano and H. Pagels, *Phys.Rept.* **36**, 137 (1978).
- [75] J. Taylor, *Nucl.Phys.* **B33**, 436 (1971).
- [76] M. Q. Huber and L. von Smekal, *JHEP* **06**, 015 (2014).
- [77] J. S. Ball and T.-W. Chiu, *Phys.Rev.* **D22**, 2542 (1980).
- [78] J. S. Ball and T.-W. Chiu, *Phys.Rev.* **D22**, 2550 (1980).
- [79] C. S. Fischer and R. Alkofer, *Phys.Rev.* **D67**, 094020 (2003).